The American Journal of Pathology, Vol. 173, No. 5, November 2008

DOI: 10.2353/ajpath.2008.071177

Cell Injury, Repair, Aging and Apoptosis

Overexpression of mIGF-1 in Keratinocytes Improves Wound Healing and Accelerates Hair Follicle Formation and Cycling in Mice

Ekaterina Semenova,* Heidi Koegel,† Sybille Hasse,‡ Jennifer E. Klatte,‡§ Esfir Slonimsky,* Daniel Bilbao,* Ralf Paus,‡ Sabine Werner,† and Nadia Rosenthal*

From the European Molecular Biology Laboratory Mouse Biology Unit, Campus "A. Buzzati-Traverso," Monterotondo-Scalo, Rome, Italy; the Department of Biology,† Institute of Cell Biology, Eidgenossische Technische Hochschule Zurich, Zurich, Switzerland; the Department of Dermatology,‡ University Hospital Schleswig-Holstein, University of Luebeck, Luebeck, Germany; and the Department of Molecular Medicine,§ Max-Planck-Institute for Biochemistry, Martinsried, Germany*

Insulin-like growth factor 1 (IGF-1) is an important regulator of growth, survival, and differentiation in many tissues. It is produced in several isoforms that differ in their N-terminal signal peptide and C-terminal extension peptide. The locally acting isoform of IGF-1 (mIGF-1) was previously shown to enhance the regeneration of both muscle and heart. In this study, we tested the therapeutic potential of mIGF-1 in the skin by generating a transgenic mouse model in which mIGF-1 expression is driven by the keratin 14 promoter. IGF-1 levels were unchanged in the sera of hemizygous K14/mIGF-1 transgenic animals whose growth was unaffected. A skin analysis of young animals revealed normal architecture and thickness as well as proper expression of differentiation and proliferation markers. No malignant tumors were formed. Normal homeostasis of the putative stem cell compartment was also maintained. Healing of full-thickness excisional wounds was accelerated because of increased proliferation and migration of keratinocytes, whereas inflammation, granulation tissue formation, and scarring were not obviously affected. In addition, mIGF-1 promoted late hair follicle morphogenesis and cycling. To our knowledge, this is the first work to characterize the simultaneous, stimulatory effect of IGF-1 delivery to keratinocytes on two types of regeneration processes within a single mouse model. Our analysis supports the use of mIGF-1 for skin and hair regeneration and describes a potential cell type-restricted action. ***(Am J Pathol 2008, 173:1295–1310; DOI: 10.2353/ajpath.2008.071177)***

Insulin-like growth factor 1 (IGF-1) is a peptide hormone that promotes growth, survival, and differentiation of cells in various organs and tissues, including skin.[1,2] The importance of IGF-1 signaling in the skin is evident from the original studies with IGF-1 receptor null (*Igf-1r*$^{-/-}$) mice, which exhibited hypotrophic skin with reduced number and size of the hair follicles.[3] Similarly, deficiency in human growth hormone or its target IGF-1 are associated with decreased epidermal thickness and sparse hair growth.[4,5] Although generally recognized as a proliferation and survival factor for the skin, IGF-1 was recently also implicated in hair and skin morphogenesis.[6,7] In the skin, its levels must be strictly controlled because overexpression of IGF-1 in proliferating and in differentiating keratinocytes resulted in hyperplasia and tumor formation.[8,9]

In addition to its role in skin homeostasis, several studies suggest a role of IGF-1 in skin repair. Its expression is modulated during wound healing, and retarded healing has been correlated with reduced IGF-1 levels.[10–13] *In vitro*, IGF-1 was shown to stimulate keratinocyte proliferation and migration, as well as collagen production by fibroblasts.[14–17] Consequently, local administration of IGF-1 to wound sites enhanced wound closure and stimulated granulation tissue formation.[18,19] On the other hand, increased IGF-1 receptor expression was reported in chronic wounds and in hypertrophic scars, and IGF-1 stimulation was associated with increased invasive ca-

Supported by a Marie Curie Incoming International Fellowship (to E.S.), the European Union (Ulcer Therapy LSHB-CT-2005-512102 grant to N.R. and S.W.), and the Deutsche Forschungsgemeinschaft (grant Pa 345/12-1 to R.P.).

Accepted for publication July 18, 2008.

Supplemental material for this article can be found on *http://ajp.amjpathol.org.*

Address reprint requests to Dr. Ekaterina Semenova, European Molecular Biology Laboratory (EMBL)-Mouse Biology Unit, Via Ramarini 32, Monterotondo-Scalo, 00015 Roma, Italy. E-mail: ekat@embl.it.

pacity of keloid fibroblasts.[20,21] In addition, systemic delivery of IGF-1 with the goal to improve wound healing caused hyperglycemia, electrolyte imbalance, and edema.[22,23]

IGF-1 is also implicated in the control of hair cycling, a regenerative process that constantly occurs in the skin. *In vitro*, IGF-1 maintained hair follicles in a growth phase (anagen), and removal of IGF-1 led to a catagen-like regression.[24] Transgenic animals, in which an ultra-high-sulfur keratin gene promoter was used to target IGF-1 to the wool follicles of the sheep or hair follicles of the mouse, showed increased fleece weight and vibrissae length, respectively.[25,26] Hair appeared earlier in transgenic mice overexpressing IGF-1 in the skin under control of the keratin 1 (K1) promoter.[8] In contrast, hair follicles of transgenic mice expressing IGF-1 in the skin under control of the involucrin promoter, showed a delay in anagen entry.[7] This difference could result from different promoter usage, but also from the use of different IGF-1 isoforms.

IGF-1 is produced in multiple isoforms that differ in their amino-terminal signal peptides and carboxy-terminal extension peptide.[27] Previous studies[28,29] and preliminary results from our laboratory suggest that the isoform determines localization and may define the mode of IGF-1 action. In muscle and heart regeneration studies using transgenic models, the outcome of regeneration depended on the isoform used.[30,31] This stresses the importance of both IGF-1 isoform selection and the mode of delivery in preclinical regeneration studies and in therapeutic application of this growth factor.

In the skin, IGF-1 is produced by cells of mesenchymal origin, such as fibroblasts of the dermis and dermal papilla, whereas its receptor is produced by both mesenchymal and epithelial cells.[32–35] Thus, keratinocytes respond to the paracrine signal originating from the neighboring mesenchymal cells. We set out to test whether providing a localized autocrine signal to epithelial cells, including basal keratinocytes of interfollicular epidermis and outer root sheath (outer root sheath) keratinocytes of the hair follicle, can enhance wound repair and hair regeneration without causing deleterious effects, such as increased scarring, tumor formation, and systemic imbalance. To this end, we generated transgenic mice expressing a locally acting form of IGF-1 (mIGF-1[36]) under the control of the keratin 14 promoter. These studies identify mIGF-1 as a potent stimulator of hair follicle morphogenesis and cycling, and of re-epithelialization of skin wounds. Importantly, these effects are not accompanied by spontaneous malignant tumor formation and occur in the background of normal epidermal homeostasis.

Materials and Methods

Cloning of the Transgene Construct and Generation of Transgenic Mice

The mIGF-1 rat cDNA was amplified from an MLC/*mIgf-1* cassette[36] with primers containing *Bam*HI sites: the forward primer was 5′-CGGGATCCCTGTTTCCTGTCTACAGTGTC-3′ and the reverse primer was 5′-CGGGATCCCTCGGGAGGCTCCTCCTAC-3′. The polymerase chain reaction (PCR) product was analyzed by sequencing and cloned into the *Bam*HI site located downstream of the β-globin intron in the pG3Z.K14 cassette (kindly provided by Dr. Elaine Fuchs, Rockefeller University, New York, NY).[37] The pG3Z.K14 cassette includes a 2-kb *Ava*I fragment of the human K14 promoter followed by a 700-bp β-globin intron and 500 bp of the human K14 polyadenylation signal (poly A). The transgene fragment was excised using *Kpn*I upstream of the K14 promoter and *Hind*III downstream of the K14 poly A. The fragment was gel-purified and microinjected into male pronuclei of FVB zygotes. Founders were crossed with wild-type FVB animals and positive progeny were maintained in a hemizygous state. Genotyping, using tail genomic DNA as a template, was performed by PCR using standard conditions and two sets of PCR primers. The first set is located within the human K14 poly A sequence: 5′-GTGTGGACACAGATCCCAC-3′ and 5′-GGAGACACCACATATGACC-3′. The second set is located within exons 3 and 4 of the rat IGF-1 sequence: 5′-TTCCTGTCTACAGTGTCTGTG-3′ and 5′-GAGCTGACTTTGTAGGCTTCA-3′. Animals were housed in a clean, temperature-controlled mouse facility on a 12-hour light/dark cycle, and standard diet was provided. All mouse procedures were approved by the European Molecular Biology Laboratory Monterotondo Ethical Committee (Monterotondo, Italy) and were in accordance with national and European regulations. Eight- to ten-week-old sex-matched male and female animals (unless otherwise specified) were used for the study.

Northern Blotting and in Situ *Analysis*

Total RNA was extracted using TRIzol Reagent (Invitrogen, Carlsbad, CA). For Northern blot analysis, 15 μg of total RNA for each sample were blotted and hybridized using standard conditions. *In situ* hybridization was performed as previously described.[38] A probe corresponding to the complete rat mIGF-1 cDNA described above was used for both Northern blotting and *in situ* hybridization.

Immunoenzymometric Assay

To determine circulating IGF-1 levels, the OCTEIA rat/mouse IGF-1 immunoenzymometric assay for the quantitative determination of IGF-1 in rat and mouse serum was used according to the manufacturer's instructions (IDS Limited, Frankfurt, Germany).

Histological Analysis

For histological analysis, upper back skin was isolated, fixed overnight in 4% paraformaldehyde in phosphate-buffered saline (PBS), and embedded in paraffin. Dewaxed sections (7 μm) were stained using hematoxylin

and eosin (H&E) and photographed using a Leica DC 500 camera (Leica Microsystems, Wetzlar, Germany).

Detection of Proliferating Cells by Labeling with 5-Bromo-2′-Deoxyuridine (BrdU)

Mice were injected intraperitoneally with BrdU (250 mg/kg BrdU in 0.9% NaCl) and sacrificed 2 hours after injection. Back skin and wound sections were fixed overnight in acetic ethanol (1% acetic acid/95% EtOH) and incubated with a horseradish peroxidase-conjugated monoclonal antibody directed against BrdU (Roche, Basel, Switzerland). BrdU-positive cells were visualized using 3,3-diaminobenzidine substrate (Sigma, St. Louis, MO). Counterstaining was performed with H&E.

Analysis of the Ki-67-Positive Keratinocytes within the Hair Follicle

Upper back skin sections fixed in 4% buffered formalin were stained with the anti-Ki-67 antibody (Novocastra, Newcastle upon Tyne, UK). All Ki-67$^+$ cells and the total number of matrix keratinocytes below the Auber's line were counted in morphogenesis stage 8 on day 8 after birth and in anagen on day 28 after birth. Seven to thirteen individual hair follicles derived from three different mice per group were counted (mean ± SEM, $*P < 0.05$), analyzed by Mann-Whitney test for unpaired samples (GraphPad Prism; GraphPad Software Inc., San Diego, CA). All Ki-67$^+$ cells of the outer root sheath in the visual field above the hair bulb were counted at a magnification of ×200 in morphogenesis stage 8 on day 8 after birth and in anagen on day 28 after birth. Twelve individual HFs derived from three different mice per group were counted (mean ± SEM, $*P < 0.05$ for day 8, $*P < 0.0001$ for day 28, analyzed by Mann-Whitney test for unpaired samples).

Transwell Migration Assay

Migration assay was performed using transwell migration chambers (6.5 mm diameter, 8-μm pore size) (Costar; Corning, Lowell, MA) in 24-well plates. In all of the experiments, cell adhesion was achieved by precoating the transwell with vitrogen 100 collagen (Cohesion Technologies, Palo Alto, CA) and fibronectin (Invitrogen). Primary keratinocytes were isolated from 3-day-old pups as described.[39] After 2 days in culture, keratinocytes were trypsinized and seeded at 1×10^4 cells in 200 μl of Dulbecco's modified Eagle's medium per upper chamber. Six hundred μl of Dulbecco's modified Eagle's medium or of Dulbecco's modified Eagle's medium supplemented with 1% chelated serum were added to the lower chamber. Cells were allowed to migrate for 4 hours after which nonmigrated cells were removed from the top of the filter. The filter was stained in 20% methanol/0.1% crystal violet, mounted, and the whole filter was photographed using a Leica DMRx microscope (with ×5 objective) and a Leica DFC290 digital camera. Keratinocytes from three to four wild-type and transgenic animals were pooled and each assay was performed in triplicates. The total number of migrated cells was counted for each filter. The data presented are a mean of triplicate experiments ± SD. Statistical analysis was performed using the unpaired *t*-test with GraphPad Prism software. The migration experiment was repeated with three different litters.

Affymetrix Microarray Analysis

Wounds were generated as described above. Wound samples, including clot and 2 mm of the surrounding skin were collected 24 hours after wounding. Seven to fourteen wounds from five wild-type and five transgenic animals were split into three groups per genotype and thus a total of six groups were subjected to Affymetrix array analysis (Affymetrix, Santa Clara, CA). Gene expression in wound skin samples was determined using Mouse Genome 430 2.0 arrays (Affymetrix). Each sample was hybridized to an individual microarray chip. Target preparation, hybridization, and scanning were conducted according to the Affymetrix GeneChip Expression technical manual by Gene Core facility (EMBL, Heidelberg, Germany). Data files were analyzed using GeneSpring 7.3 software (Silicon Genetics, Redwood City, CA). Briefly, Affymetrix data were imported into GeneSpring software and normalized by using the default normalization methods recommended by the software. Lists of differentially expressed transcripts were generated by using a one-way analysis of variance parametric test and a *P* value cutoff of 0.05. Additional stringent filtering criteria were applied to comparative analyzes, including filter on flags, volcano plot, presence of the signal in three of three replicates. Venn diagrams were generated to identify differentially regulated transcripts. Additionally, the gene list of cytokines, chemokines, and growth factors containing GenBank ID and the fold expression change was generated manually.

Immunofluorescence

Seven-μm sections from the middle of the acidic ethanol-fixed wounds or from back skin were deparaffinized, rehydrated, rinsed in PBS, and incubated overnight at 4°C with the primary antibodies diluted in PBS containing 1% bovine serum albumin and 0.01% Nonidet P-40. After three 10-minute washes with PBS/0.1% Tween 20, the sections were incubated for 1 hour at room temperature with the Cy2- or Cy3-coupled secondary antibodies (Jackson ImmunoResearch Laboratory Inc., West Grove, PA), washed, mounted with Mowiol (Hoechst, Frankfurt, Germany), and analyzed with a Zeiss Axioplan fluorescence microscope (Zeiss, Oberkochen, Germany). The following antibodies were used: a mouse monoclonal antibody directed against keratin 10 (1:100; DAKO, Glostrup, Denmark), rabbit polyclonal antibodies directed against keratin 14 (1:5000; Babco, Richmond, CA), keratin 6 (1:1000, Babco), and loricrin (1:250; Covance, Denver, PA).

Fluorescence-Activated Cell Sorting (FACS) Analysis

Back skin from wild-type and transgenic 47 dpp male animals was used for the analysis as described previously.[40] Primary antibodies used for flow cytometric analysis were anti-α6 integrin (CD49f) directly coupled to phycoerythrin and anti-CD34 directly coupled to fluorescein isothiocyanate (BD Pharmingen, Franklin Lakes, NJ). Dead cells were stained with 7-AAD (Sigma) and excluded from the analysis. Analysis was performed in a three laser standard configuration FACS Aria (BD Biosciences, San Jose, Ca). Data analysis was performed using FACS Diva (BD Biosciences) and FlowJo software (Tree Star, Inc., Ashland, OR). Compensation was performed manually after acquisition of 110,000 events. Gating of the putative stem cell populations was performed as indicated in figure legend.

Wound Healing

Four full-thickness excisional wounds, 5 mm in diameter, were made on either side of the dorsal midline of 8- to 10-week-old mice by excising skin and panniculus carnosus. Wounds were left uncovered and harvested 5, 14, and 21 days after injury. Mice were housed individually during the healing period. For histological analysis the complete wounds including 2 mm of the epithelial margins were isolated, bisected, fixed overnight in 4% paraformaldehyde in PBS (for Masson trichrome analysis) or in acetic ethanol (for immunofluorescence and BrdU staining), and embedded in paraffin. Sections (7 μm) from the middle of the wound were stained using the Masson's trichrome procedure as described by the manufacturer (Sigma) and photographed using a Leica DC 500 camera (Leica Microsystems). Morphometric measurements of the wounds were performed on both BrdU- and Masson's trichrome-stained sections using the OpenLab software (Improvision Ltd., Basel, Switzerland). Wound-healing experiments (excisional and incisional wounds; see below) were performed with permission from the local veterinary authorities of Zurich, Switzerland. Statistical analysis was performed using the unpaired *t*-test (given the variances were normally distributed) included in the GraphPad Prism4 software package.

Wound Bursting Strength

Mice were anesthetized and the dorsal region was shaved and treated with a depilatory agent (Pilca Perfect; Stafford-Miller Continental, Oevel, Belgium). Four full-thickness incisions (1 cm) were made at two anterior and two posterior dorsal sites, and the skin margins were closed with strips of wound plaster (Fixomull stretch; Beiersdorf, Hamburg, Germany). Mice were sacrificed on day 5 after wounding, and bursting strength of the wounds was determined *in situ* using the BTC-2000 system (SRLI Technologies, Nashville, TN) according to the manufacturer's protocol for the nonhuman disruptive linear incision analysis.

Hair Type Analysis

Hair was plucked from five wild-type and five transgenic 28 dpp male animals and at least 200 single hair shafts per animal were analyzed to determine the percentage of each hair type. Hair shafts were analyzed using a Leica MZ12 stereo microscope, photographed using a Leica DC 500 camera, and hair shaft length was measured using MetaMorph7 software (Molecular Devices Corp., Sunnyvale, CA).

Quantitative Histomorphometry of Hair Follicles

Skin samples of K14/mIGF-1 mice and their wild-type littermates were harvested from the back at 1, 8, 17, 28, and 49 days post partum (dpp). This allows to reliably assess differences in early morphogenesis (dpp 1), late morphogenesis (dpp 8), as well as the entry into hair follicle cycling (dpp 17, first catagen), and in subsequent hair cycling activity (dpp 28, first anagen; dpp 49, second telogen).[41,42] For cryosectioning, skin samples were embedded as described elsewhere[42] and 6-μm sections were prepared and stained with Giemsa. At each time point, histomorphometric analysis was performed on 25 to 100 hair follicles derived from three different mice per group (mean $\pm$ SEM, $^{***}P < 0.0001$, $^{*}P < 0.05$). Statistical analysis was performed using the Mann-Whitney test for unpaired samples included in the GraphPad Prism4 software package. Presented analysis was performed on transgenic line F, similar results were obtained for line C (data not shown). Hair cycle stages were determined and grouped as described elsewhere.[41,42]

Results

Generation and Initial Characterization of K14/mIGF-1 Transgenic Mice

A locally acting isoform of IGF-1 (mIGF-1), which comprises a class 1 signal peptide, derived from exon 1 and an Ea extension peptide derived from exons 4 and 6, was shown to improve muscle and heart regeneration.[30,36] To test whether the production of mIGF-1 by keratinocytes can improve cutaneous wound repair and to study its effect on hair follicle morphogenesis and cycling, we generated transgenic mice that express mIGF-1 ectopically under the control of a human K14 promoter fragment (Figure 1A).[37] Three independent transgenic lines were established of which two were chosen for further analysis. Mice from line C had a higher level of expression compared to those from line F (Figure 1B). As expected, transgene expression was detected in the skin but not in the liver or heart (Figure 1C). *In situ* hybridization confirmed the expected K14 promoter-driven expression of the mIGF-1 transgene in the K14-positive cells of the basal layer of the epidermis and in the outer

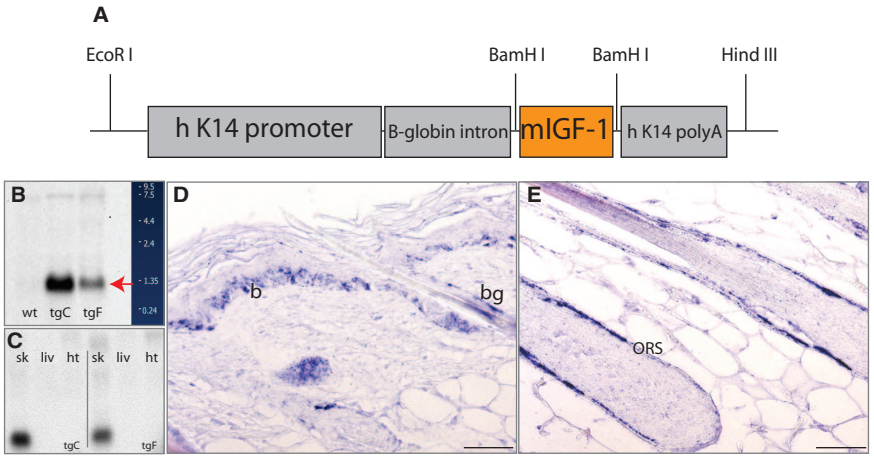

Figure 1. K14/mIGF-1 construct and transgene expression. **A:** Schematic representation of the of K14/mIGF-1 expression cassette. **B:** Northern blot analysis of total skin RNA samples using a rat mIGF-1 cDNA probe shows the transgene-derived mRNA (**red arrow**) in the highest expressing line tg C and in the lower expressing line tg F. No transgene-derived transcript is detectable in the wild-type skin sample. **C:** Northern blot analysis of total RNA from skin (sk), liver (liv), and heart (ht), using the human K14 poly A probe, shows that expression of the transgene is skin-specific in both transgenic lines C and F. **D** and **E:** Nonradioactive *in situ* hybridization of sections from adult back skin of a transgenic animal (line C) with a rat mIGF-1 cDNA probe shows expression of the transgene in the basal layer of the epidermis (b) and in the bulge region (bg) and the outer root sheath of the hair follicle (outer root sheath). Original magnifications, ×40.

root sheath and the bulge compartment of the hair follicles (Figure 1, D and E).

From analysis of other transgenic models, mIGF-1 is predicted to remain at or near the site of production, and therefore should not lead to side effects and secondary phenotypes resulting from an increase in circulating IGF-1 levels.[30,36] Accordingly, the level of total free IGF-1 was similar in the serum from wild-type (411.7 ± 12.14 ng/ml) and K14/mIGF-1 transgenic mice (405.2 ± 10.31 ng/ml) (Figure 2A). In addition, we monitored the growth of wild-type mice and transgenic littermates, and did not detect accelerated growth or increased weight in adult transgenic animals (Figure 2B). Interestingly, we noticed a slight deceleration in the growth of transgenic animals during the weaning period that can result from an inability to efficiently switch from milk to solid food that could be caused by K14 promoter-driven mIGF-1 expression in the tongue or oral mucosa.[43] The average weight of livers and hearts from wild-type and transgenic mice was similar (Figure 2, C and D).

Transgenic mice of both lines were viable and fertile and generally appeared normal with no clearly visible skin or hair alterations. The earliest macroscopic phenotype observed in both mIGF-1 transgenic lines was an enlargement of the ear surface in K14/mIGF-1 mice (Figure 2E) and earlier appearance of the hair (data not shown). The ear phenotype was first visible ~4 to 5 dpp, with the ear surface of transgenic mice being 30% larger compared to that of the wild-type mice. In adulthood, ears of transgenic mice were 25% larger. This phenotype was maintained throughout the mouse lifespan and allowed for easy identification of transgenic animals. At the age of 4 to 6 months, 80% of transgenic mice developed a cataract-like eye phenotype (Figure 2, F and G), likely caused by K14-driven mIGF-1 expression in the cornea of the eye.[44] The severity of this phenotype was lower in line F, suggesting a dose dependency.

mIGF-1 Does Not Affect Skin Morphogenesis and Homeostasis in Young Mice

To assess the effect of K14-driven mIGF-1 on skin morphogenesis and homeostasis, we performed histological characterization of back and tail skin from 7-week-old wild-type and K14/mIGF-1 transgenic mice. The thickness and general architecture of the epidermis, dermis, and hypodermis appeared normal in the transgenic mice (Figure 3, A and B). Because IGF-1 is known to stimulate cell proliferation, we analyzed the effect of mIGF-1 expression by keratinocytes on their proliferation. For this purpose, we injected mice with BrdU 2 hours before sample collection and stained back and tail skin sections

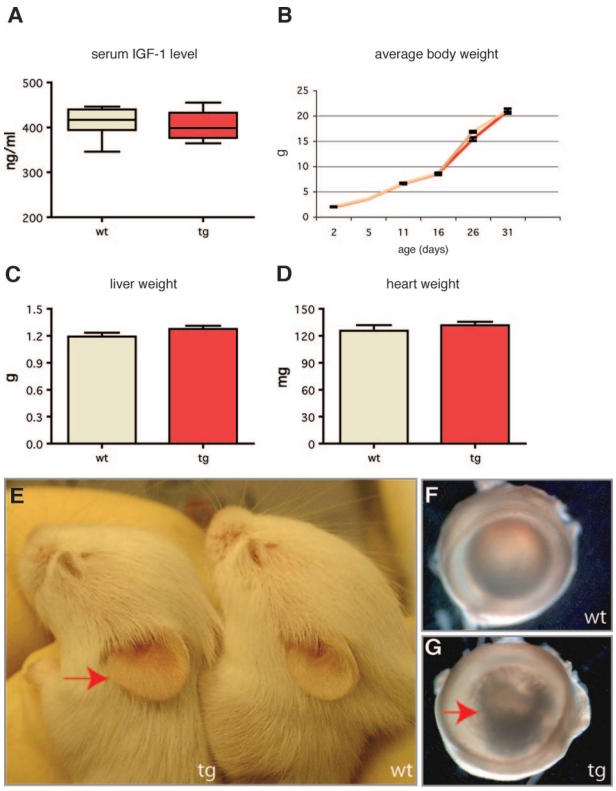

Figure 2. Initial phenotypic characterization of K14/mIGF-1 mice. **A:** Serum levels of IGF-1, measured by IGF-1 immunoenzymometric assay, are similar ($P = 0.69$) in wild-type ($n = 8$) and transgenic mice ($n = 9$). **B:** Growth curves of wild-type (yellow) ($n = 16$) and transgenic (red) ($n = 14$) animals show a similar pattern. **C** and **D:** Liver and heart weights are similar ($P = 0.1$ and $P = 0.4$, respectively) in wild-type and transgenic mice. **E:** Transgenic mice (10 dpp) have enlarged ears (**red arrow**). **F:** Normal eye in a wild-type mouse (**G**) and eye from a transgenic mouse with a cataract (**red arrow**).

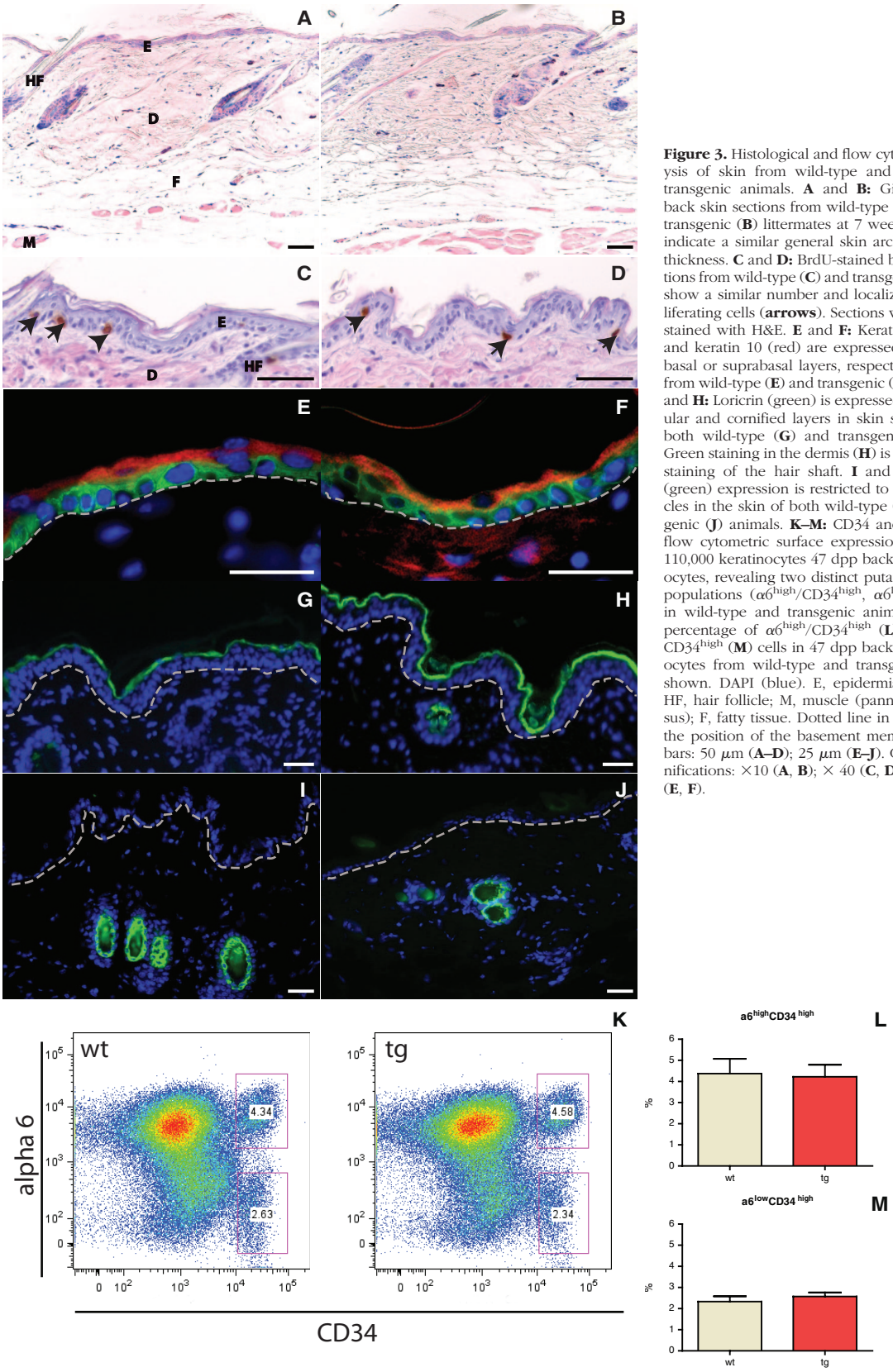

Figure 3. Histological and flow cytometric analysis of skin from wild-type and K14/mIGF-1 transgenic animals. **A** and **B:** Giemsa-stained back skin sections from wild-type mice (**A**) and transgenic (**B**) littermates at 7 weeks after birth indicate a similar general skin architecture and thickness. **C** and **D:** BrdU-stained back skin sections from wild-type (**C**) and transgenic (**D**) mice show a similar number and localization of proliferating cells (**arrows**). Sections were counterstained with H&E. **E** and **F:** Keratin 14 (green) and keratin 10 (red) are expressed properly in basal or suprabasal layers, respectively, of skin from wild-type (**E**) and transgenic (**F**) animals. **G** and **H:** Loricrin (green) is expressed in the granular and cornified layers in skin samples from both wild-type (**G**) and transgenic (**H**) mice. Green staining in the dermis (**H**) is a nonspecific staining of the hair shaft. **I** and **J:** Keratin 6 (green) expression is restricted to the hair follicles in the skin of both wild-type (**I**) and transgenic (**J**) animals. **K–M:** CD34 and $\alpha 6$ integrin flow cytometric surface expression analysis of 110,000 keratinocytes 47 dpp back skin keratinocytes, revealing two distinct putative stem cell populations ($\alpha 6^{high}/CD34^{high}$, $\alpha 6^{low}/CD34^{high}$) in wild-type and transgenic animals (**K**). The percentage of $\alpha 6^{high}/CD34^{high}$ (**L**) and $\alpha 6^{low}/CD34^{high}$ (**M**) cells in 47 dpp back skin keratinocytes from wild-type and transgenic mice is shown. DAPI (blue). E, epidermis; D, dermis; HF, hair follicle; M, muscle (panniculus carnosus); F, fatty tissue. Dotted line in **E–J** indicates the position of the basement membrane. Scale bars: 50 μm (**A–D**); 25 μm (**E–J**). Original magnifications: ×10 (**A**, **B**); × 40 (**C**, **D**, **H–J**); ×100 (**E**, **F**).

with an anti-BrdU antibody. This analysis showed a similar number of basal proliferating cells in the back and tail epidermis in samples from wild-type (16 cells per mm basement membrane) and transgenic (15 cells per mm basement membrane) mice (Figure 3, C and D; and data not shown). To address the possible effect of mIGF-1 expression on the homeostatic regulation of the skin stem cell compartment, we isolated keratinocytes from the back skin of 3-week-old and 7-week-old male wild-type and transgenic animals and assayed the number of putative basal ($\alpha6^{high}CD34^{high}$) and suprabasal ($\alpha6^{low}CD34^{high}$) bulge stem cells by flow cytometric analysis.[40] No significant difference was detected, indicating that mIGF-1 expression does not perturb homeostasis of the bulge compartment (Figure 3, K–M; and data not shown).

To study the effect of mIGF-1 on keratinocyte differentiation, we analyzed the expression of differentiation-specific proteins in back skin sections of wild-type and K14/mIGF-1 transgenic mice. In normal epidermis, keratin 14 is restricted to the basal layer of the epidermis, whereas cells in the suprabasal layers express keratin 10. Both keratin 14 (green) and keratin 10 (red) showed a normal pattern of expression (Figure 3, E and F). Loricrin, a major protein of the cornified envelope, was also properly expressed in the granular and cornified layers of the epidermis of K14/mIGF-1 transgenic mice (Figure 3, G and H). Keratin 6 expression is restricted to hair follicles of normal skin but is expressed in interfollicular epidermis of neoplastic, hyperplastic, and psoriatic skin.[45] We did not detect keratin 6 outside of the hair follicle compartment in K14/mIGF-1 transgenic skin (Figure 3, I and J). Thus K14 promoter-driven expression of mIGF-1 did not disturb early skin homeostasis, and the process of keratinocyte differentiation was not affected.

Wound Re-Epithelialization Is Accelerated in K14/mIGF-1 Transgenic Mice and the Stromal Component Is Not Affected

We next tested whether mIGF-1, at a dose that does not perturb epidermal homeostasis, is sufficient to stimulate regenerative events in the skin. We first assessed its effect on the wound healing process. Previous studies suggested an important role of IGF-1 in wound healing.[46] However, because of variability in the mode of delivery and possibly the isoforms used, the phenotypes ranged from intra-epidermal to systemic, resulting in adverse side effects.[18,22,46–48] To test the effect of K14 promoter-driven mIGF-1 expression on wound re-epithelialization and remodeling, 5-mm full-thickness excisional wounds were generated on the back of wild-type and K14/mIGF-1 transgenic age- and sex-matched animals.

To follow the healing process, we performed a detailed histomorphometric analysis at day 5, day 14, and day 21 after wounding, using sections from the middle of the wounds. At day 5, wounds undergo active re-epithelialization and granulation tissue formation.[46] To analyze 5-day wounds, two independent wounding experiments were performed with a total of 11 transgenic and 10 wild-type animals. Nine wounds from the wild-type and thirteen wounds from the transgenic animals were sectioned, and sections from the middle of the wounds were stained using the Masson's trichrome method, which allowed for clear visual characterization of both dermal and epidermal components. Five of thirteen wounds in transgenic animals were fully closed, compared to one of nine wounds in the wild-type mice. We calculated the average diameter of the open wound. This parameter, measured as the distance between migrating edges of epithelial tongues (Figure 4, A, B, E, and F; arrows), was 0.7 mm in the wounds of transgenic animals and 1.6 mm in the wounds of wild-type mice (Figure 4J). Thus, the efficiency of wound closure was strongly enhanced in K14/mIGF-1 animals.

Wound closure is influenced by both re-epithelialization and wound contraction. To estimate the contribution of wound contraction, we measured the distance between the wound edges, which were identified by the location of the most proximal hair follicles on either side of the wound (Figure 4, A, B, E, and F; arrowheads). Although wound contraction was increased by 10% in the wounds of transgenic animals, this difference was not statistically significant at this stage (Figure 4, A, B, E, and F; and data not shown). To estimate the efficiency of re-epithelialization, we measured the percentage of wound closure (percentage of distance covered by epidermis between the wound edges; Figure 4, A, B, E, and F). The percentage of wound closure was equal to 55% in the wounds of wild-type animals and 82% in the wounds of the transgenic animals (Figure 4K). Thus, increased re-epithelialization was mainly responsible for the more efficient wound closure in transgenic animals.

The accelerated re-epithelialization could be a result of increased proliferation or migration of keratinocytes. To identify the effect of mIGF-1 overexpression on proliferation of wound keratinocytes, we measured the area of hyperproliferative epithelium (Figure 4, A–I; labeled as HE). The latter was increased by 65% in the wounds of transgenic mice (179,300 $\pm$ 8546 μm^2 compared to 108,900 $\pm$ 5169 μm^2 in the wild-type) (Figure 4L). To determine the role of keratinocyte proliferation at day 5 after wounding, we injected BrdU 2 hours before wound collection. The total number of proliferating (BrdU-positive) cells within the area of hyperproliferative epithelium was significantly higher in the wounds of transgenic animals (175 $\pm$ 26 compared to 119 $\pm$ 12 in the wounds of wild-type animals) (Figure 4M), indicating an ongoing hyperproliferation. If mIGF-1 had an additional effect on keratinocyte migration, it would be reflected in the length of the wound epithelium, which includes hyperproliferative epidermis and the migrating tongue. In fact, the length of the wound epithelium was increased by 60% in the transgenic wounds (Figure 4, A–I and N). These findings suggest that mIGF-1 expression by keratinocytes promoted keratinocyte proliferation as well as migration in wounded skin, thus allowing for the more rapid and efficient wound closure.

Accelerated re-epithelialization in our mIGF-1 transgenic mice might result from a direct effect of mIGF-1 on keratinocytes or from an indirect effect that is mediated via the stroma. In the early phase of the repair process,

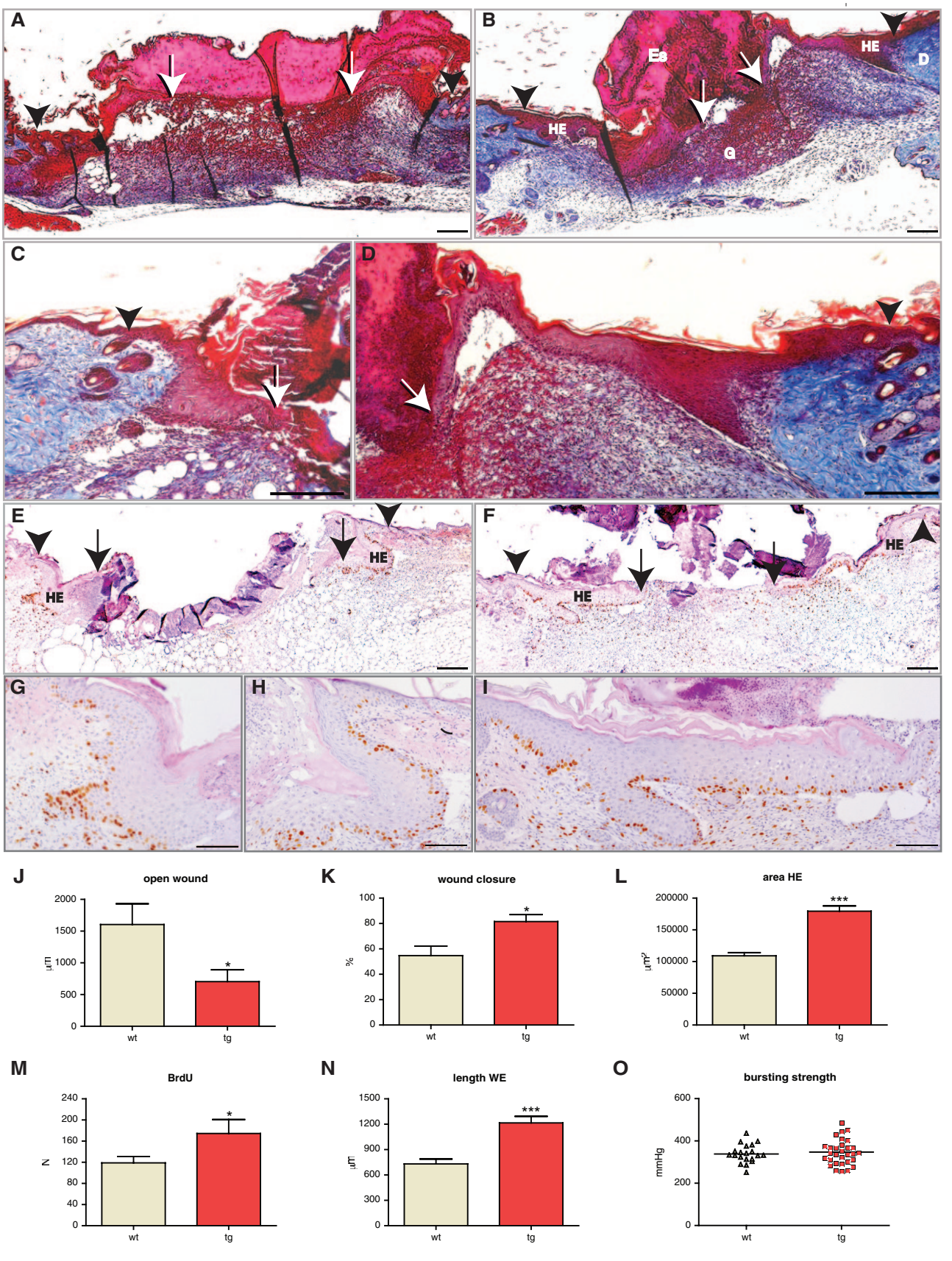
A
B
HE
D
HE
G
C
D
E
HE
HE
F
HE
HE
G
H
I
J
open wound
µm
2000
1500
1000
500
0
*
wt
tg
K
wound closure
%
100
80
60
40
20
0
*
wt
tg
L
area HE
µm²
200000
150000
100000
50000
0
***
wt
tg
M
BrdU
N
240
200
160
120
80
40
0
*
wt
tg
N
length WE
µm
1500
1200
900
600
300
0
***
wt
tg
O
bursting strength
mmHg
600
400
200
0
wt
tg

inflammatory cells are particularly important regulators of keratinocyte migration and proliferation.[46,49] To assess the possible effect of mIGF-1 on the early inflammatory response, we collected wounds 24 hours after wounding and performed Affymetrix expression profiling analysis. No significant differences were detected in the expression of various chemokines, cytokines, and growth factors that are known to be associated with the inflammatory response in the wound (Supplemental Table 1, available at *http://ajp.amjpathol.org*). To analyze the inflammatory infiltrate in the wounds at a later stage of healing, we stained 5-day wounds with antibodies that detect neutrophils or macrophages, and quantified the number of infiltrating cells. This analysis, similarly, revealed no significant differences between mIGF-1 and wild-type animals (data not shown). We also did not observe a significant difference in vascularization, collagen deposition, or cellularity of the granulation tissue at 5 days after wounding (Figure 4, A–D). To analyze the maturation stage of the granulation tissue we performed a wound-bursting strength experiment. Four full-thickness 1-cm incisions were made on the back of 11 wild-type and 10 K14/mIGF-1 transgenic animals (35 and 36 wounds, respectively). Bursting strength of the wounds was measured at day 5 after wounding, when incisional wounds are fully re-epithelialized. Changes in connective tissue composition and collagen cross-linking alter the vacuum needed to break the wound. Normal unwounded skin has higher bursting strength compared to wound tissue because of extensive collagen cross-linking of normal dermis. In line with our histological findings, the median bursting strength was similar in wounds from wild-type and K14/mIGF-1 transgenic mice (Figure 4O). In summary, the above data suggest that the stimulatory effect of K14 promoter-driven mIGF-1 is restricted to the epithelial component of the skin, affecting mainly the re-epithelialization aspect of the healing process.

mIGF-1 Does Not Adversely Affect the Quality of the Healed Wound

We subsequently analyzed wounds at later stages to determine the effect of continuous expression of mIGF-1 by keratinocytes on wound maturation. Excisional wounds were generated on the back of six wild-type and six K14/mIGF-1 transgenic age-matched animals, and wound tissue was collected 14 days after wounding. A total of nine wounds for each genotype was fully sectioned and characterized. All wounds were closed at this time point. The location of the most proximal hair follicles identified the outer margins of the wounds (Figure 5, A–D; arrowhead), and the length of the epidermis between the wound margins was measured to determine the wound width. Wounds from transgenic mice were 20% smaller compared to those from wild-type animals (Figure 5, A–D and E), reflecting enhanced wound contraction. The most striking difference however, was the dramatic increase in the thickness of epithelium covering the wounds of K14/mIGF1 transgenic animals, with an average thickness of 155 μm in transgenic mice compared to 65 μm in the wild-type mice (Figure 5, A–D and F). In addition, three of nine wounds of transgenic animals contained epidermal cysts (Figure 5D, red arrow). To check whether this increase in the epidermal thickness was accompanied by altered keratinocyte redifferentiation in the wound epithelium, we stained sections taken from the middle of wounds with antibodies against early and late differentiation markers. Keratinocyte differentiation was found to be normal in wounds from K14/mIGF-1 transgenic mice with keratin 14 (Figure 5, G and H; red), keratin 10 (Figure 5, G and H; green), and loricrin (Figure 5, I and J; green) showing normal distribution. Similar to the 5-day time point, the area and density of granulation tissue in the transgenic mice was comparable to that of wild-type animals (Figure 5, A–D).

To test whether the acanthosis seen in the 14-day transgenic wound epithelium is resolved, wounds were generated on the back of five wild-type and five transgenic animals and collected after 21 days. A total of 10 wounds from wild-type mice and 9 wounds from transgenic mice were analyzed. Sections from the middle of the wounds were stained using the Masson's trichrome method. Wounds from wild-type and transgenic mice appeared similar, with thin epithelium covering the complete wound bed. Epidermal cysts were no longer visible. Granulation tissue, although larger in total area (1.35 mm^2 in wounds of transgenic mice compared to 0.96 mm^2 in wounds of wild-type mice) showed similar cellularity and collagen density as well as similar general architecture (Figure 6, A–C). In summary, expression of the local isoform of mIGF-1 by keratinocytes accelerated wound closure while allowing for normal collagen deposition with no signs of pathological scarring.

The Effect of K14-Driven mIGF-1 Expression on Hair Morphology, Hair Follicle Morphogenesis, and Cycling

Given its pronounced effect on wound healing, it was likely that K14-driven mIGF-1 expression would also

Figure 4. Accelerated wound closure in K14/mIGF-1 transgenic mice is driven by an increase in keratinocyte proliferation and migration. Ten wild-type animals (9 wounds) and eleven transgenic animals (13 wounds) were analyzed. **A** and **B:** Masson's trichrome-stained sections from the center of 5-day wounds of wild-type (**A**) and transgenic (**B**) animals are shown. **C** and **D:** Enlarged images of Masson trichrome-stained sections taken from the center of 5-day wounds of wild-type (**C**) and transgenic (**D**) mice, showing the hyperproliferative epithelium (HE). **E** and **F:** BrdU-stained sections from the center of 5-day wounds of wild-type (**E**) and transgenic (**F**) animals. **G–I:** Enlarged images of the hyperproliferative epithelium from BrdU-stained wound sections of wild-type (**G** and **H**) and transgenic (**I**) animals. BrdU-stained sections were counterstained with H&E. **J:** Average diameter of the open wound ($P = 0.0207$); **K:** percent wound closure ($P = 0.0124$); **L:** area of HE ($P < 0.0001$); **M:** number of BrdU-positive cells within the hyperproliferative epithelium (HE) ($P = 0.0414$); and **N:** length of the wound epithelium (WE) ($P < 0.0001$) are shown. **O:** Wound bursting strength is plotted as a negative force in mmHg required to break the wound. Eleven wild-type animals (35 wounds) and ten transgenic animals (36 wounds) were assayed in the wound-bursting strength experiment. G, granulation tissue; D, dermis; Es, eschar. **White Arrows** indicate the foremost tips of the epithelial tongues. **Black Arrowheads** indicate the wound edges. Scale bars: 200 μm (**A–F**); 100 μm (**G–I**). Original magnifications: ×10 (**A**, **B**, **E**, **F**); ×20 (**C**, **D**, **G–I**).

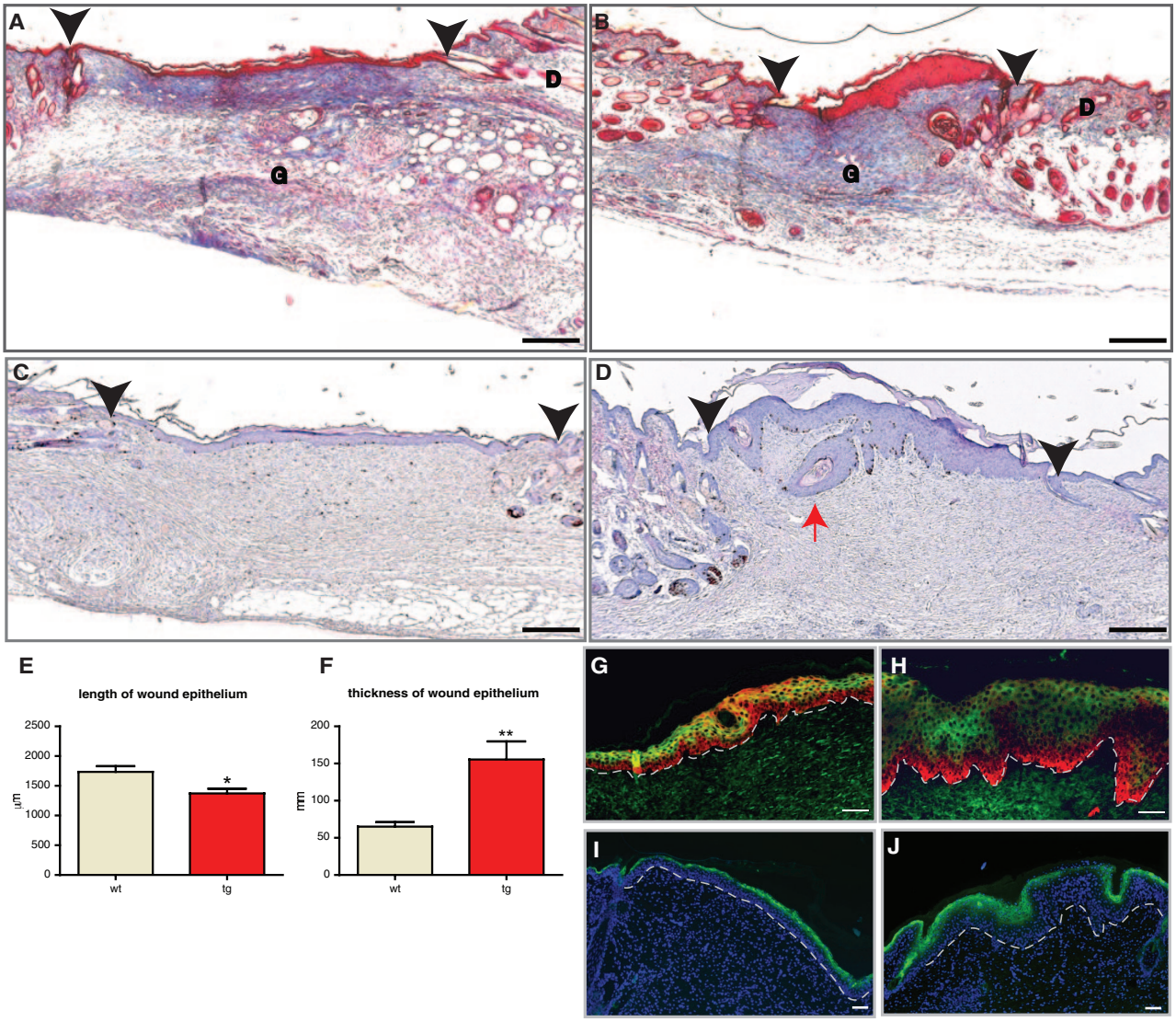

Figure 5. Reduced size, hyperthickened epithelium, and normal epidermal differentiation in 14-day excisional wounds. Six wild-type and six transgenic animals (nine wounds for each genotype) were analyzed. **A** and **B:** Masson trichrome-stained sections from the middle of representative 14-day excisional wounds of wild-type (**A**) and transgenic (**B**) animals are shown. Granulation tissue (G) and dermis (D) are indicated. **C** and **D:** BrdU-stained sections from the middle of representative 14-day wounds of wild-type (**C**) and transgenic (**D**) animals are shown. **Black arrowheads** indicate the edges of the original wound. The **red arrow** points to an epidermal cyst. **E:** Graphic representation of the average length of wound epithelium (*$P = 0.0099$). **F:** Graphic representation of the average thickness of wound epithelium (**$P = 0.0014$). **G** and **H:** Immunofluorescence staining of the 14-day wound epithelium in wild-type (**G**) and transgenic (**H**) mice, using a keratin 14 antibody (red) and a keratin 10 antibody (green). **I** and **J:** Immunofluorescence staining of 14-day wound epithelium from wild-type (**I**) and transgenic (**J**) mice, stained with a loricrin antibody (green) and DAPI (blue). **Dotted line** identifies the location of a basement membrane. Scale bars: 200 μm (**A–D**); 50 μm (**G–J**). Original magnifications: ×10 (**A–D**); ×20 (**G–J**).

affect hair follicle morphogenesis and cycling, which shares many mechanistic and molecular events with wound healing.[50–52] The hair follicle undergoes cyclic transformations from phases of rapid growth (anagen), via apoptosis-driven regression (catagen), to relative rest (telogen). At the onset of a new growth phase, keratinocytes in the bulge region, a putative stem cell compartment, proliferate and migrate into the dermis to regenerate the lower two-thirds of the follicle.[52,53] This anagen-associated regeneration is reminiscent of the events that occur during wound repair. In both cases keratinocytes proliferate, rearrange the expression of adhesion receptors, secrete proteases and collagenases, and migrate. In fact, hair follicle depilation, which induces a pronounced wound-healing response of the follicle, represents the strongest known stimulus for inducing a telogen-anagen switch in hair follicle cycling.[52] On wounding, bulge cells move upward and can contribute to wound re-epithelialization,[54] whereas the connective tissue sheath of the hair follicle is likely to provide key cellular input into granulation tissue formation, angiogenesis, and nerve fiber remodeling during wound healing.[51]

In the hair follicle, K14 is expressed by the outer root sheath, a layer continuous with the basal layer of the epidermis, whereas IGF-1 is expressed mainly by cells of mesenchymal origin (dermal papilla). The IGF-1 receptor is expressed by both epithelial and mesenchy-

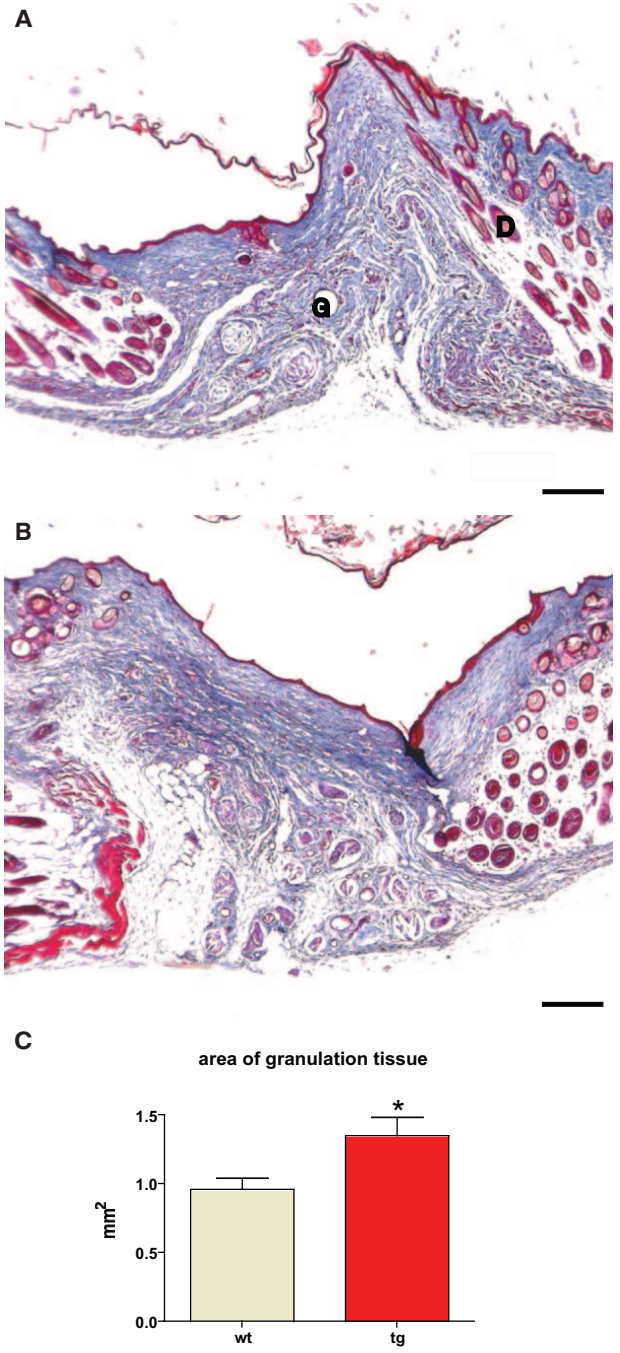

Figure 6. Normal epithelial thickness and general granulation tissue architecture in 21-day excisional wounds. **A** and **B:** Masson trichrome staining of representative sections from the middle of 21-day excisional wounds taken from wild-type (**A**) and transgenic (**B**) mice. Granulation tissue (G) and dermis (D) are indicated. Five wild-type animals (10 wounds) and five transgenic animals (9 wounds) were analyzed. **C:** The area of granulation tissue (*$P = 0.0205$) is shown. Scale bars = 200 μm. Original magnifications, ×10.

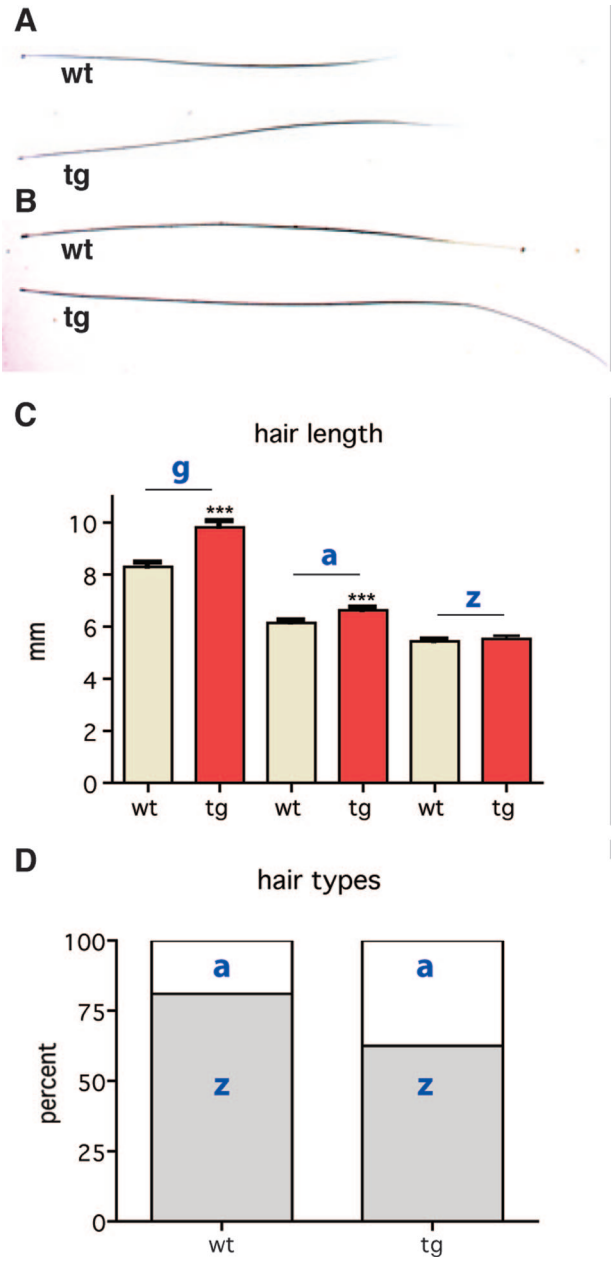

Figure 7. The effect of K14-driven mIGF-1 expression on the hair coat. **A** and **B:** Awl and guard hair shafts are shown. **C:** Transgenic guard hairs (g) are elongated by 20% (***$P > 0.0001$), transgenic awl hairs (a) are elongated by 10% (***$P > 0.001$), whereas zigzag hair (z) length is not changed. **D:** The frequencies of zigzag (z) and awl (a) hairs in wild-type mice are 79% and 21%, respectively, and in transgenic mice they are 60% and 40%, respectively.

mal cells. By targeting mIGF-1 to the K14-expressing cells, we created a novel autocrine activation of IGF-1 signaling in outer root sheath cells.

We first analyzed the integrity of the hair coat in K14/mIGF-1 transgenic mice. Mice have four different hair types (guard, awl, auchene, and zigzag), which can be distinguished according to their length, shape, and internal structure.[55] The hair of the equivalent upper-dorsal area of wild-type and K14/mIGF-1 transgenic mice was removed, measured, and classified according to specific type. Although all four types of hair were present in transgenic animals, the frequencies of each type were altered. In the wild-type mice, the percentages of zigzag and awl hairs were 79% and 21%, respectively, whereas in the coat of transgenic mice they were 60% and 40%, respectively (Figure 7D). In both wild-type and K14/mIGF-1 transgenic animals, guard hairs represented ~2% of all hairs. Hair length was also affected

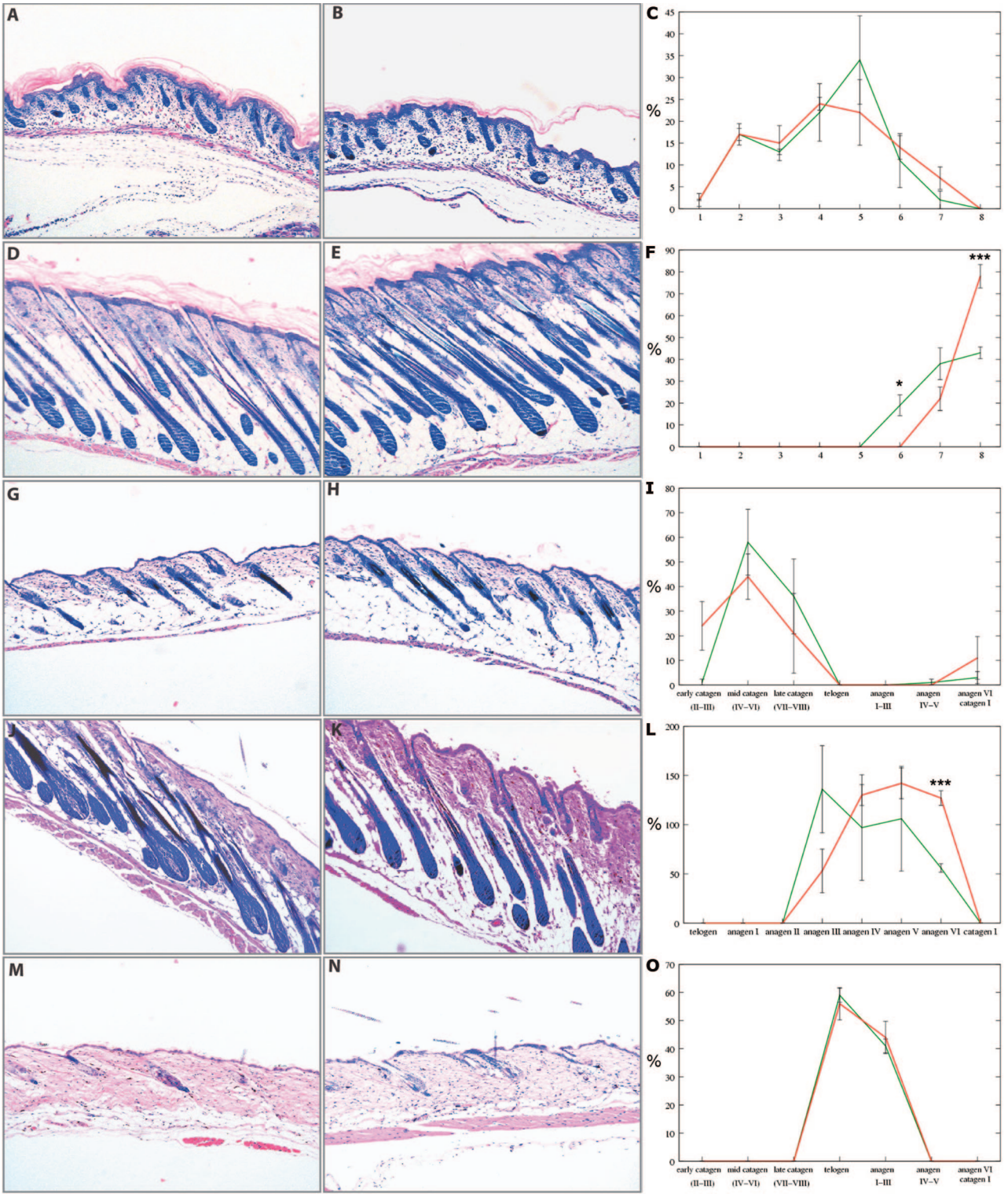

Figure 8. mIGF-1 accelerates late hair follicle morphogenesis and anagen development. Giemsa staining of back skin sections from wild-type (**A**, **D**, **G**, **J**, **M**) and transgenic (**B**, **E**, **H**, **K**, **N**) mice is shown. **C**, **F**, **I**, **L**, and **O:** Quantitative analysis of hair follicles from wild-type (green) and transgenic (red) mice in various stages of morphogenesis and cycling. $^{*}P \geq 0.05$ and $^{***}P \geq 0.001$. **A–C:** One dpp, early morphogenesis. **D–F:** Eight dpp, late morphogenesis. **G–I:** Seventeen dpp, early catagen. **J–L:** Twenty-eight dpp, anagen. **M–O:** Forty-nine dpp, telogen. X-axes in **C** and **F** identify nine distinct hair follicle morphogenesis stages. X-axes in **I**, **L**, and **O** identify distinct stages of hair follicle cycling. Y-axes show the percentage of hair follicles in each distinct stage of hair follicle morphogenesis or cycling. Original magnifications, ×10.

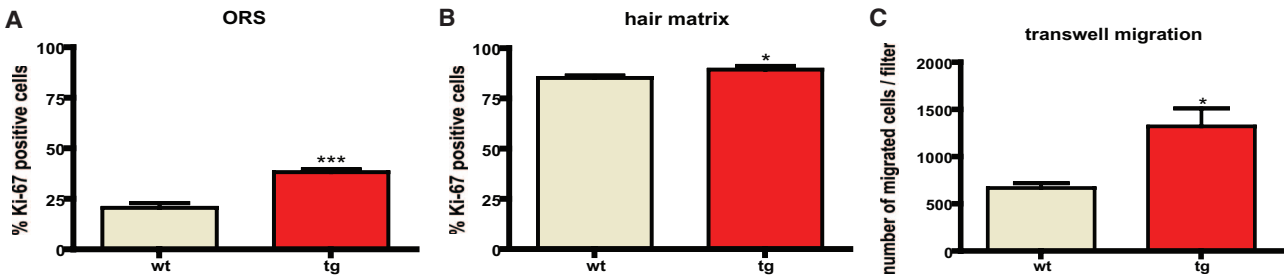

Figure 9. The effect of mIGF-1 on hair follicle keratinocyte proliferation *in vivo* and primary keratinocyte migration *in vitro*. **A:** The percentage of Ki-67-positive keratinocytes in the outer root sheath of the anagen hair follicle on day 28 (***$P < 0.0001$) is shown. **B:** The percentage of Ki-67-positive keratinocytes in the matrix of anagen hair follicle bulbs on day 28 (*$P < 0.05$) is shown. **C:** The average number of cells, migrated through a transwell insert (6.5 mm in diameter) within 4 hours (mean ± SEM; *$P < 0.05$) is shown.

in K14/mIGF-1 transgenic mice with 10% longer awl hairs and 20% longer guard hairs compared to the wild-type (Figure 7, A–C). No difference in the length of zigzag hairs was found. Macroscopic analysis did not reveal any gross abnormalities in the hair structure.

To analyze the hair cycle progression, we collected dorsal skin at 1 dpp (early morphogenesis), 8 dpp (late morphogenesis), 17 dpp (catagen), 28 dpp (anagen), and 49 dpp (telogen) from wild-type and K14/mIGF-1 transgenic sex-matched littermates and analyzed hair follicles by quantitative histomorphometry. Because mouse hair cycling occurs in waves, standardized longitudinal sections from an identical location on the back of the mice were used for the analysis.[56] The percentage of hair follicles at each stage of morphogenesis or cycling was calculated and summarized in the graphs (Figure 8, C, F, I, L, and O). These data were used to determine the hair cycle stage at each time point. Hair follicle cycling induces profound alterations in skin thickness, with the dramatic increase in anagen and concomitant decrease in telogen.[41,42] Therefore, skin thickness provided an additional parameter for the stage of the hair cycle.

On day 1, the hair follicles of the wild-type and K14/mIGF-1 transgenic animals were very similar in development (Figure 8C). Although the wild-type mice had more hair follicles in stage 5 compared to transgenic animals, the difference was not significant. In support of this result, skin thickness was similar between wild-type and K14/mIGF-1 transgenic animals (Figure 8, A and B). On day 8, transgenic mice had significantly more hair follicles in the more advanced, stage 8, of hair follicle morphogenesis, whereas wild-type mice had significantly more hair follicles in stage 6 (Figure 8F). Increased skin thickness supported the histomorphometric findings (Figure 8, D and E). These results showed a clear promotion of late hair follicle morphogenesis in K14/mIGF-1 transgenic mice.

On day 17, murine hair follicles enter the first catagen phase, thereby initiating hair follicle cycling. At that time point, hair follicles of the wild-type mice were already in mid and late catagen, whereas K14/mIGF-1 transgenic hair follicles were still in late morphogenesis and early catagen (Figure 8I). Although these data were not statistically significant, skin of transgenic animals was thicker, corroborating the histomorphometric data and pointing to a delay in catagen entry (Figure 8, G and H). We next analyzed the anagen stage of the first hair cycle (day 28). Similar to late morphogenesis, we observed a clear acceleration of anagen development, and the curve for K14/mIGF-1 transgenic mice was shifted to the right (Figure 8L). There were significantly more anagen III hair follicles in wild-type mice and significantly more anagen VI follicles in K14/mIGF-1 transgenic mice (Figure 8L). As expected from these data, skin of transgenic mice, being in the more advanced anagen, was thicker (Figure 8, J and K). At day 49, hair follicles from both wild-type and transgenic mice were in telogen and in early anagen (Figure 8O). This was also reflected in a similar skin thickness (Figure 8, M and N). Thus, in contrast to IGF-1 expression under the involucrin promoter, K14-driven mIGF-1 accelerated late hair follicle morphogenesis and cycling while possibly delaying catagen entry.[7]

To test whether mIGF-1 stimulates hair morphogenesis and cycling by affecting proliferation of hair follicle keratinocytes, we stained sections taken from day 8 and day 28 dorsal skin of wild-type and transgenic animals with a Ki-67 antibody that marks proliferating cells. We documented a strong and significant increase in the number of Ki-67-positive cells in the outer root sheath (Figure 9A and data not shown), and a weaker but significant increase in the number of proliferating cells within the matrix compartment (Figure 9B and data not shown). These results implicate increased proliferation as one of the mechanisms of mIGF-1 action on hair growth.

We propose that mIGF-1 can act in an autocrine manner on the keratinocytes that secrete it. To test whether mIGF-1 can enhance keratinocyte migration through an autocrine signaling, we performed an *in vitro* keratinocyte migration assay in a transwell setting. Primary keratinocytes were isolated from wild-type and transgenic neonatal animals and plated on a collagen/fibronectin-coated plates. After 2 days in culture, cells were collected and an equal number was plated on top of the transwell inserts. Cells were allowed to migrate for 4 hours and the number of migrated cells was quantified. We observed a clear acceleration of migration in keratinocytes isolated from K14/mIGF-1 transgenic animals, with more than a 100% increase in the number of migrated cells (Figure 9C). Thus, mIGF-1 is capable of stimulating both wound healing and hair regeneration

processes and its mechanism of action is likely to involve an autocrine/paracrine stimulation of keratinocyte proliferation and migration.

Discussion

The IGF-1 system has been implicated in wound healing, and expression of its components is modulated during the healing process.[46] Conversely, compromised wound healing has been associated with deregulation of IGF-1 signaling.[12,13] Similar to wound healing, hair growth and regeneration involve proliferation, migration, and differentiation of keratinocytes. It has also been associated with IGF-1 action[57] because mice carrying a null mutation in the *Igf-1r* gene exhibited reduced number and size of the hair follicles.[3] Here we show that expression of a locally acting IGF-1 isoform (mIGF-1) is capable of enhancing skin and hair regeneration without perturbing epidermal differentiation and early homeostasis. The K14/mIGF-1 transgene used in this study is likely to promote both skin regeneration and hair growth through autocrine stimulation of the keratinocytes by which it is expressed.

Different modes of IGF-1 delivery have been tested in wound healing models with varying results. Systemic delivery of IGF-1 was not efficient in treating incisional wounds in rats, whereas GH delivery increased wound strength and was correlated with increased intensity of IGF-1 immunostaining in the granulation tissue, implicating locally produced IGF-1 as a mediator of GH action.[47] In another experiment, wound healing in transgenic mice with greatly elevated postnatal serum GH and IGF-1 levels exhibited severe healing abnormalities that included delayed wound closure because of an increase in granulation tissue formation and inefficient wound contraction.[58] In general, when delivered systemically, IGF-1 might lead to hypoglycemia, electrolyte imbalance, and fatigue, in particular because supraphysiological doses are needed to enhance healing.[22] In contrast, no systemic effects were reported on a local delivery of IGF-1 cDNA under a CMV promoter by subcutaneous liposomal gene transfer to burn wounds in rat.[18] This treatment resulted in enhanced re-epithelialization, increased collagen deposition by fibroblasts, and an increased number of newly formed blood vessels, thus stimulating both epidermal and dermal components.[18] Here we report an enhancement of wound healing through a local effect of mIGF-1 on epidermal proliferation and migration, not accompanied by major alterations in the underlying dermis/granulation tissue. Because IGF-1 may lead to excessive scarring by overstimulating fibroblast proliferation, migration, and collagen deposition at the wound site,[16,59,60] targeted delivery of a locally acting IGF-1 isoform to keratinocytes, as in the present study, may be necessary to avoid negative side effects on other skin cell types.

To obtain a comprehensive picture of the mIGF-1 effect on regeneration, we analyzed hair follicle morphogenesis and cycling, a spontaneously occurring physiological regeneration and remodeling event closely related to wound healing. Our analysis of the hair cycle in K14/mIGF-1 animals shows that hair follicles in the transgenic skin are progressing through late morphogenesis and anagen of the first hair cycle with a higher rate and are likely to remain longer in anagen, as indicated by a possible delay in catagen entry. As expected, these alterations result in elongation of the guard and awl hair shafts in the skin of K14/mIGF-1 transgenic mice. In the previous *in vivo* studies, additional IGF-1 was supplied by differentiated noncycling cells of the hair follicle,[25,26] and the suggested mechanism of growth enhancement involved either stimulation of the follicular metabolism, or the ability of IGF-1 to diffuse into the follicular bulb and to stimulate proliferation of the actively cycling matrix cells. Transgenic mice overexpressing IGF-1 under a keratin 1 promoter showed earlier hair appearance,[8] and this effect is also likely to involve IGF-1 diffusion or activation of other cell types in the skin. In our model, mIGF-1 is expressed in the basal layer of the outer root sheath that incorporates the stem cell compartment and thus the autocrine stimulation of their proliferation and migration should directly lead to enhanced follicle growth. Interestingly, and in contrast to our results, IGF-1 driven by the involucrin promoter leads to a delay in anagen entry, although elongation of guard hair is observed.[7] Because the promoters and the IGF-1 isoforms used in the two studies are different, it is difficult to speculate on the likely cause of these alternative observations. The present study further underscores a strong connection between the two regeneration types, in which mIGF-1 may stimulate and assist regenerative phases through autocrine stimulation of keratinocyte migration and proliferation. The localized nature of the stimulatory effect has particular clinical relevance.

Tight modulation of growth factor levels is likely to be a critical factor in the design of IGF-1 therapies for wound healing and hair regeneration. In this regard, histological evaluation of the K14/mIGF-1 transgenic mouse skin did not reveal abnormalities in keratinocyte proliferation or differentiation in 7-week-old mice, whereas mice expressing the human homologue of mIGF-1 under the bovine keratin 5 promoter (BK5.IGF-1) exhibited epidermal hyperplasia and hyperkeratosis at 8 weeks and 50% of BK5.IGF-1 mice developed spontaneous tumors (some of which converted to squamous cell carcinomas) between 6 to 12 months.[9] In contrast, no malignant tumors were formed in K14/mIGF-1 transgenic animals. In the first generation of heterozygous transgenic animals, 4 of 16 transgenic mice developed four (one per animal) benign tumors, at the age of 14 months or later. However, tumor formation did not re-occur in the next generations of aging (between 14 and 22 months of age) transgenic mice (0 of 27 transgenic animals to date), suggesting that their presence was related to secondary genetic background effects that were eliminated in subsequent generations. The absence of malignant tumors in this model is an unexpected finding, given the highly proliferative nature of the skin and the suggested role of IGF-1 in tumor biology.[61–68] Thus, we show that mIGF-1 can be delivered to the skin and hair at a physiological level that does not disturb homeostasis and avoids malignant tumor formation, while at the same time stimulating two

different, but strongly related regenerative processes through a localized effect on keratinocyte proliferation and migration.

Maintaining normal homeostasis of the bulge is essential for proper hair cycling and is implicated in efficient wound healing and prevention of uncontrolled growth.[69–71] Depletion of the skin stem cell compartment results in impaired wound healing and hair loss,[72] whereas its expansion can predispose skin to cancer.[73,74] Our analysis of the bulge compartment using α6 and CD34 markers shows that mIGF-1, produced by the stem cells and by the outer root sheath cells, does not perturb homeostasis of the bulge in 7-week-old unwounded skin. Preliminary analysis of the label-retaining cell compartment in wild-type and K14/mIGF-1 transgenic animals supports this conclusion (data not shown). However, with additional signals, such as those that emanate from the wound site or from the dermal papilla at the onset of anagen, mIGF-1 is likely to modify the behavior of stem cells and their progeny by possibly increasing their proliferation, migration, or reducing apoptosis and thus enhancing both wound healing and hair regeneration. Analyzing the status of the skin stem cells and transit amplifying cells at different stages of the hair cycle, during wound healing and in aging, will shed light on the mechanisms and contribute to the development of stem cell-mediated IGF-1-based regenerative therapies.

Acknowledgments

We thank Jose Gonzalez and Valeria Berno for technical help, Emerald Perlas for technical help and stimulating discussions, Dr. Philippe Bugnon for performing the tensile strength experiments, Dr. Francisco Jose Bilbao for histopathological characterization of tumor samples, and Dr. Saveria Pastore for critical consideration of this work.

References

1. Dupont J, Holzenberger M: Biology of insulin-like growth factors in development, Birth Defects Res C Embryo Today 2003, 69:257–271
2. Edmondson SR, Thumiger SP, Werther GA, Wraight CJ: Epidermal homeostasis: the role of the growth hormone and insulin-like growth factor systems. Endocr Rev 2003, 24:737–764
3. Liu JP, Baker J, Perkins AS, Robertson EJ, Efstratiadis A: Mice carrying null mutations of the genes encoding insulin-like growth factor I (Igf-1) and type 1 IGF receptor (Igf1r). Cell 1993, 75:59–72
4. Lange M, Thulesen J, Feldt-Rasmussen U, Skakkebaek NE, Vahl N, Jorgensen JO, Christiansen JS, Poulsen SS, Sneppen SB, Juul A: Skin morphological changes in growth hormone deficiency and acromegaly. Eur J Endocrinol 2001, 145:147–153
5. Lurie R, Ben-Amitai D, Laron Z: Laron syndrome (primary growth hormone insensitivity): a unique model to explore the effect of insulin-like growth factor 1 deficiency on human hair. Dermatology 2004, 208:314–318
6. Sadagurski M, Yakar S, Weingarten G, Holzenberger M, Rhodes CJ, Breitkreutz D, Leroith D, Wertheimer E: Insulin-like growth factor 1 receptor signaling regulates skin development and inhibits skin keratinocyte differentiation. Mol Cell Biol 2006, 26:2675–2687
7. Weger N, Schlake T: Igf-I signalling controls the hair growth cycle and the differentiation of hair shafts, J Invest Dermatol 2005, 125:873–882
8. Bol DK, Kiguchi K, Gimenez-Conti I, Rupp T, DiGiovanni J: Overexpression of insulin-like growth factor-1 induces hyperplasia, dermal abnormalities, and spontaneous tumor formation in transgenic mice. Oncogene 1997, 14:1725–1734
9. DiGiovanni J, Bol DK, Wilker E, Beltran L, Carbajal S, Moats S, Ramirez A, Jorcano J, Kiguchi K: Constitutive expression of insulin-like growth factor-1 in epidermal basal cells of transgenic mice leads to spontaneous tumor promotion. Cancer Res 2000, 60:1561–1570
10. Gartner MH, Benson JD, Caldwell MD: Insulin-like growth factors I and II expression in the healing wound, J Surg Res 1992, 52:389–394
11. Vogt PM, Lehnhardt M, Wagner D, Jansen V, Krieg M, Steinau HU: Determination of endogenous growth factors in human wound fluid: temporal presence and profiles of secretion. Plast Reconstr Surg 1998, 102:117–123
12. Blakytny R, Jude EB, Martin Gibson J, Boulton AJ, Ferguson MW: Lack of insulin-like growth factor 1 (IGF1) in the basal keratinocyte layer of diabetic skin and diabetic foot ulcers. J Pathol 2000, 190:589–594
13. Brown DL, Kane CD, Chernausek SD, Greenhalgh DG: Differential expression and localization of insulin-like growth factors I and II in cutaneous wounds of diabetic and nondiabetic mice. Am J Pathol 1997, 151:715–724
14. Ando Y, Jensen PJ: Epidermal growth factor and insulin-like growth factor I enhance keratinocyte migration. J Invest Dermatol 1993, 100:633–639
15. Daian T, Ohtsuru A, Rogounovitch T, Ishihara H, Hirano A, Akiyama-Uchida Y, Saenko V, Fujii T, Yamashita S: Insulin-like growth factor-I enhances transforming growth factor-beta-induced extracellular matrix protein production through the P38/activating transcription factor-2 signaling pathway in keloid fibroblasts. J Invest Dermatol 2003, 120:956–962
16. Granot I, Halevy O, Hurwitz S, Pines M: Growth hormone and insulin-like growth factor I regulate collagen gene expression and extracellular collagen in cultures of avian skin fibroblasts. Mol Cell Endocrinol 1991, 80:1–9
17. Haase I, Evans R, Pofahl R, Watt FM: Regulation of keratinocyte shape, migration and wound epithelialization by IGF-1- and EGF-dependent signalling pathways. J Cell Sci 2003, 116:3227–3238
18. Jeschke MG, Schubert T, Klein D: Exogenous liposomal IGF-I cDNA gene transfer leads to endogenous cellular and physiological responses in an acute wound. Am J Physiol Regul Integr Comp Physiol 2004, 286:R958–966
19. Jyung RW, Mustoe JA, Busby WH, Clemmons DR: Increased wound-breaking strength induced by insulin-like growth factor I in combination with insulin-like growth factor binding protein-1. Surgery 1994, 115:233–239
20. Ghahary A, Shen YJ, Wang R, Scott PG, Tredget EE: Expression and localization of insulin-like growth factor-1 in normal and post-burn hypertrophic scar tissue in human. Mol Cell Biochem 1998, 183:1–9
21. Yoshimoto H, Ishihara H, Ohtsuru A, Akino K, Murakami R, Kuroda H, Namba H, Ito M, Fujii T, Yamashita S: Overexpression of insulin-like growth factor-1 (IGF-I) receptor and the invasiveness of cultured keloid fibroblasts. Am J Pathol 1999, 154:883–889
22. Bondy CA, Underwood LE, Clemmons DR, Guler HP, Bach MA, Skarulis M: Clinical uses of insulin-like growth factor I. Ann Intern Med 1994, 120:593–601
23. Jabri N, Schalch DS, Schwartz SL, Fischer JS, Kipnes MS, Radnik BJ, Turman NJ, Marcsisin VS, Guler HP: Adverse effects of recombinant human insulin-like growth factor I in obese insulin-resistant type II diabetic patients. Diabetes 1994, 43:369–374
24. Philpott MP, Sanders DA, Kealey T: Effects of insulin and insulin-like growth factors on cultured human hair follicles: IGF-I at physiologic concentrations is an important regulator of hair follicle growth in vitro. J Invest Dermatol 1994, 102:857–861
25. Damak S, Su H, Jay NP, Bullock DW: Improved wool production in transgenic sheep expressing insulin-like growth factor 1. Biotechnology (NY) 1996, 14:185–188
26. Su HY, Hickford JG, The PH, Hill AM, Frampton CM, Bickerstaffe R: Increased vibrissa growth in transgenic mice expressing insulin-like growth factor 1. J Invest Dermatol 1999, 112:245–248
27. Adamo ML, Neuenschwander S, LeRoith D, Roberts CT, Jr.: Structure, expression, and regulation of the IGF-I gene. Adv Exp Med Biol 1993, 343:1–11
28. Barton ER: Viral expression of insulin-like growth factor-I isoforms promotes different responses in skeletal muscle. J Appl Physiol 2006, 100:1778–1784

29. Goldspink G: Gene expression in skeletal muscle. Biochem Soc Trans 2002, 30:285–290
30. Santini MP, Tsao L, Monassier L, Theodoropoulos C, Carter J, Lara-Pezzi E, Slonimsky E, Salimova E, Delafontaine P, Song YH, Bergmann M, Freund C, Suzuki K, Rosenthal N: Enhancing repair of the mammalian heart. Circ Res 2007, 100:1732–1740
31. Shavlakadze T, Winn N, Rosenthal N, Grounds MD: Reconciling data from transgenic mice that overexpress IGF-I specifically in skeletal muscle. Growth Horm IGF Res 2005, 15:4–18
32. Hodak E, Gottlieb AB, Anzilotti M, Krueger JG: The insulin-like growth factor 1 receptor is expressed by epithelial cells with proliferative potential in human epidermis and skin appendages: correlation of increased expression with epidermal hyperplasia. J Invest Dermatol 1996, 106:564–570
33. Little JC, Redwood KL, Granger SP, Jenkins G: In vivo cytokine and receptor gene expression during the rat hair growth cycle. Analysis by semi-quantitative RT-PCR. Exp Dermatol 1996, 5:202–212
34. Rudman SM, Philpott MP, Thomas GA, Kealey T: The role of IGF-I in human skin and its appendages: morphogen as well as mitogen? J Invest Dermatol 1997, 109:770–777
35. Tavakkol A, Elder JT, Griffiths CE, Cooper KD, Talwar H, Fisher GJ, Keane KM, Foltin SK, Voorhees JJ: Expression of growth hormone receptor, insulin-like growth factor 1 (IGF-1) and IGF-1 receptor mRNA and proteins in human skin. J Invest Dermatol 1992, 99:343–349
36. Musaro A, McCullagh K, Paul A, Houghton L, Dobrowolny G, Molinaro M, Barton ER, Sweeney HL, Rosenthal N: Localized Igf-1 transgene expression sustains hypertrophy and regeneration in senescent skeletal muscle. Nat Genet 2001, 27:195–200
37. Vassar R, Rosenberg M, Ross S, Tyner A, Fuchs E: Tissue-specific and differentiation-specific expression of a human K14 keratin gene in transgenic mice, Proc Natl Acad Sci USA 1989, 86:1563–1567
38. Neubuser A, Koseki H, Balling R: Characterization and developmental expression of Pax9, a paired-box-containing gene related to Pax1. Dev Biol 1995, 170:701–716
39. Montanez E, Piwko-Czuchra A, Bauer M, Li S, Yurchenco P, Fassler R: Analysis of integrin functions in peri-implantation embryos, hematopoietic system, and skin. Methods Enzymol 2007, 426:239–289
40. Blanpain C, Lowry WE, Geoghegan A, Polak L, Fuchs E: Self-renewal, multipotency, and the existence of two cell populations within an epithelial stem cell niche. Cell 2004, 118:635–648
41. Muller-Rover S, Handjiski B, van der Veen C, Eichmuller S, Foitzik K, McKay IA, Stenn KS, Paus R: A comprehensive guide for the accurate classification of murine hair follicles in distinct hair cycle stages. J Invest Dermatol 2001, 117:3–15
42. Paus R, Muller-Rover S, Van Der Veen C, Maurer M, Eichmuller S, Ling G, Hofmann U, Foitzik K, Mecklenburg L, Handjiski B: A comprehensive guide for the recognition and classification of distinct stages of hair follicle morphogenesis. J Invest Dermatol 1999, 113:523–532
43. Guo L, Yu QC, Fuchs E: Targeting expression of keratinocyte growth factor to keratinocytes elicits striking changes in epithelial differentiation in transgenic mice. Embo J 1993, 12:973–986
44. Ruberte J, Ayuso E, Navarro M, Carretero A, Nacher V, Haurigot V, George M, Llombart C, Casellas A, Costa C, Bosch A, Bosch F: Increased ocular levels of IGF-1 in transgenic mice lead to diabetes-like eye disease. J Clin Invest 2004, 113:1149–1157
45. DePianto D, Coulombe PA: Intermediate filaments and tissue repair. Exp Cell Res 2004, 301:68–76
46. Werner S, Grose R: Regulation of wound healing by growth factors and cytokines. Physiol Rev 2003, 83:835–870
47. Dunaiski V, Belford DA: Contribution of circulating IGF-I to wound repair in GH-treated rats. Growth Horm IGF Res 2002, 12:381–387
48. Koshizuka S, Kanazawa K, Kobayashi N, Takazawa I, Waki Y, Shibusawa H, Shumiya S: The beneficial effects of recombinant human insulin-like growth factor-I (IGF-I) on wound healing in severely wounded senescent mice. Surg Today 1997, 27:946–952
49. Eming SA, Krieg T, Davidson JM: Inflammation in wound repair: molecular and cellular mechanisms. J Invest Dermatol 2007, 127:514–525
50. Cotsarelis G: The hair follicle: dying for attention. Am J Pathol 1997, 151:1505–1509
51. Jahoda CA, Reynolds AJ: Hair follicle dermal sheath cells: unsung participants in wound healing. Lancet 2001, 358:1445–1448
52. Stenn KS, Paus R: Controls of hair follicle cycling, Physiol Rev 2001, 81:449–494
53. Alonso L, Fuchs E: The hair cycle. J Cell Sci 2006, 119:391–393
54. Ito M, Liu Y, Yang Z, Nguyen J, Liang F, Morris RJ, Cotsarelis G: Stem cells in the hair follicle bulge contribute to wound repair but not to homeostasis of the epidermis. Nat Med 2005, 11:1351–1354
55. Dry F: Th ecoat of the mouse (*Mus musclus*). J Genet 1926, 165:281–340
56. Paus R, Cotsarelis G: The biology of hair follicles. N Engl J Med 1999, 341:491–497
57. Su HY, Hickford JG, Bickerstaffe R, Palmer BR: Insulin-like growth factor 1 and hair growth. Dermatol Online J 1999, 5:1
58. Thorey IS, Hinz B, Hoeflich A, Kaesler S, Bugnon P, Elmlinger M, Wanke R, Wolf E, Werner S: Transgenic mice reveal novel activities of growth hormone in wound repair, angiogenesis, and myofibroblast differentiation. J Biol Chem 2004, 279:26674–26684
59. Conover CA, Dollar LA, Rosenfeld RG, Hintz RL: Somatomedin C-binding and action in fibroblasts from aged and progeric subjects. J Clin Endocrinol Metab 1985, 60:685–691
60. Conover CA, Hintz RL, Rosenfeld RG: Comparative effects of somatomedin C and insulin on the metabolism and growth of cultured human fibroblasts. J Cell Physiol 1985, 122:133–141
61. Chan JM, Stampfer MJ, Giovannucci E, Gann PH, Ma J, Wilkinson P, Hennekens CH, Pollak M: Plasma insulin-like growth factor-I and prostate cancer risk: a prospective study, Science 1998, 279:563–566
62. Minuto F, Del Monte P, Barreca A, Fortini P, Cariola G, Catrambone G, Giordano G: Evidence for an increased somatomedin-C/insulin-like growth factor I content in primary human lung tumors. Cancer Res 1986, 46:985–988
63. Yee D, Paik S, Lebovic GS, Marcus RR, Favoni RE, Cullen KJ, Lippman ME, Rosen N: Analysis of insulin-like growth factor I gene expression in malignancy: evidence for a paracrine role in human breast cancer. Mol Endocrinol 1989, 3:509–517
64. Tricoli JV, Rall LB, Karakousis CP, Herrera L, Petrelli NJ, Bell GI, Shows TB: Enhanced levels of insulin-like growth factor messenger RNA in human colon carcinomas and liposarcomas. Cancer Res 1986, 46:6169–6173
65. Baserga R: The insulin-like growth factor I receptor: a key to tumor growth? Cancer Res 1995, 55:249–252
66. Sell C, Rubini M, Rubin R, Liu JP, Efstratiadis A, Baserga R: Simian virus 40 large tumor antigen is unable to transform mouse embryonic fibroblasts lacking type 1 insulin-like growth factor receptor. Proc Natl Acad Sci USA 1993, 90:11217–11221
67. Nickoloff BJ, Misra P, Morhenn VB, Hintz RL, Rosenfeld RG: Further characterization of the keratinocyte somatomedin-C/insulin-like growth factor I (SM-C/IGF-I) receptor and the biological responsiveness of cultured keratinocytes to SM-C/IGF-I. Dermatologica 1988, 177:265–273
68. Neely EK, Morhenn VB, Hintz RL, Wilson DM, Rosenfeld RG: Insulin-like growth factors are mitogenic for human keratinocytes and a squamous cell carcinoma. J Invest Dermatol 1991, 96:104–110
69. Blanpain C, Fuchs E: Epidermal stem cells of the skin. Annu Rev Cell Dev Biol 2006, 22:339–373
70. Blanpain C, Horsley V, Fuchs E: Epithelial stem cells: turning over new leaves. Cell 2007, 128:445–458
71. Ohyama M: Hair follicle bulge: a fascinating reservoir of epithelial stem cells. J Dermatol Sci 2007, 46:81–89
72. Waikel RL, Kawachi Y, Waikel PA, Wang XJ, Roop DR: Deregulated expression of c-Myc depletes epidermal stem cells. Nat Genet 2001, 28:165–168
73. Kim DJ, Chan KS, Sano S, Digiovanni J: Signal transducer and activator of transcription 3 (Stat3) in epithelial carcinogenesis. Mol Carcinog 2007, 46:725–731
74. Reya T, Morrison SJ, Clarke MF, Weissman IL: Stem cells, cancer, and cancer stem cells. Nature 2001, 414:105–111